J. Fluid. Mech. (1976), *vol.* 74, *part* 3, *pp.* 497–513
Printed in Great Britain

Density profiles in argon and nitrogen shock waves measured by the absorption of an electron beam

By H. ALSMEYER

Institut für Strömungslehre und Strömungsmaschinen,
University of Karlsruhe, Germany

(Received 14 July 1975)

Accurate measurements of the density distribution in Ar and N_2 shock waves have been made in a shock tube for the Mach number range from 1·55 to 9 and 10 respectively by the absorption of an electron beam. A modified absorption law has been used for data reduction. The density profiles were corrected for the influence of shock curvature and density rise behind the shock wave. The measurements in Ar agree to within 1 % with those of Schmidt (1969) in the mean range of M_S but give a slightly smaller density gradient for $M_S = 9$. Comparison with various theories shows very good agreement with Bird's Monte Carlo simulation in the whole Mach number range for a simple repulsive intermolecular force law. Further, the agreement with the Mott-Smith density profile for the same interaction law is also good, and surprisingly is found to be better for lower than for higher Mach numbers. Qualitative agreement is obtained with the solutions of Hicks & Yen for hard-sphere and Maxwell molecules. The Navier–Stokes and BGK solutions are found to differ significantly from the present experiments even for the lowest measured Mach number (1·55), whereas the Burnett equation gives better agreement, especially with respect to the asymmetry of the profiles.

The measured N_2 profiles agree on the whole with the shock-tube measurements of other investigators but show substantial deviations from the low density wind-tunnel experiments of Robben & Talbot (1966*b*) for higher Mach numbers. Bird's 'energy sink model' (1971) is in agreement with the measured density profiles for a realistic interaction law and a suitable rotational collision number. Rotational relaxation in nitrogen is found to be very fast for all Mach numbers. Consequently the coupling between rotational and translational relaxation is very strong.

1. Introduction

Because of the absence of boundary effects and owing to its one-dimensionality, the normal shock wave is the simplest flow with large departures from thermodynamic equilibrium. Hence the shock structure has often been investigated both experimentally and theoretically to gain a better understanding of non-equilibrium flows. Theoretical treatment of these flows is based either on continuum mechanics, i.e. the Navier–Stokes equation, or on kinetic theory, i.e. analytical or numerical solutions of the Boltzmann equation. In the last few years the kinetic-theory approach has been successfully improved by the application of different Monte Carlo methods (Bird 1971; Hicks, Yen & Reilly 1972).

In the simplest case of monatomic gases relaxation of translational energy of the molecules takes place within the shock front. For diatomic molecules, such as N_2, there is additional relaxation of the rotational degrees of freedom, which is strongly coupled to the translational relaxation. The influence of vibrational relaxation on shock structure can be neglected here. As from the microscopic point of view the flow within a shock wave is governed by molecular collision processes, the shock structure can be used to obtain information about molecular interaction laws.

To examine the predictions of different theories accurate measurements of the shock structure are required. Results of density measurements in argon and nitrogen shock waves are reported in the present work for a large Mach number range. The experimental results are compared with experimental and theoretical results of other investigators. The shock profile in Ar at the lowest measured Mach number (1·5) was found to give remarkable and perhaps unexpected results concerning the validity of the Navier–Stokes and the Mott-Smith approximation. The intermolecular force law derived from the measured shock structure reproduces the temperature dependence of shear viscosity from direct viscosity measurements.

2. Experimental technique

The experiments were performed in a conventional stainless-steel shock tube of inner diameter 150 mm. The density profile of the incoming shock wave was measured by the attenuation of an electron beam, which was located 55 diameters from the diaphragm. The arrangement was similar to that used by Schmidt (1969) in that the injection needle and the Faraday cage for the electron beam protruded into the shock tube. Thus only the central part of the shock wave was measured by the electron beam, whereas that part of the shock wave which was strongly influenced by the boundary layer and the shock curvature was not registered. The sampling length of the electron beam was 80 mm and symmetrical about the shock-tube axis. It was extended to 110 mm to study the influence of disturbances caused by the protruding parts of the apparatus. The electron beam was generated by a commercial TV electron gun. The beam current entered the shock tube through a 0·5 or 0·3 mm hole in the injection needle and was about 60 μA with 16 kV accelerating voltage. The beam was collected by a small Faraday cage.

By static calibration it was found that the attenuation of the beam current does not follow exactly the simple absorption law as was previously assumed. Additional terms have to be added taking into account (i) the influence of scattered primary electrons which are reaching the cage and (ii) backscattering from the cage. The modified absorption law for not too dense gases is given by

$$J/J_0 = A[\exp(-\alpha\rho l) + B\{1-\exp(-\alpha\rho l)\}], \tag{1}$$

where J is the beam current at the cage, J_0 the beam current entering the gas, ρ the gas density, l the sampling length of the beam and α the 'absorption' coefficient. A takes into account the backscattering from the cage and is less than unity. The term $1-\exp(-\alpha\rho l)$ represents all scattered electrons. Of these the fraction B can

reach the cage owing to small-angle scattering. B depends on the geometry of the electron-beam apparatus, mainly the diameter of the cage. In the present work A and B were 0·95 and 0·04 respectively. (For a more rigorous derivation of (1) see Alsmeyer 1974). The constants A, B and α are obtained by fitting (1) to the static calibration curves. The mean error in the calibration points was found to be less than 0·4 %.

For measurements of shock structure the cage signal was amplified and fed into an array of oscilloscopes (Tektronix 546 and 556). Two thin-film gauges were used to measure the shock speed. The initial pressure in the test section was measured with a high-precision pressure meter (MKS Baratron 90 H-1E) and varied from about 40–80 mTorr.

To improve the accuracy of the density measurements, some corrections were made to account for the non-ideal behaviour of the electronics and of the shock tube. The final rise time of the electronics (about 0·1 μs) could be eliminated on the basis of linear network theory using the measured response of the electronics to a unit step function. This correction was nearly zero for low Mach numbers and amounted to less than 3·5 % for the highest Mach numbers. Further, the measured density profiles have been corrected for the shock curvature and the small density rise behind the shock wave caused by the boundary layer on the shock tube wall. The form and justification of these corrections are discussed elsewhere (Alsmeyer 1974). The influence of the shock curvature is less than 0·6 %, whereas the influence of the density rise behind the shock wave was found to be important for the tail end of the shock wave only and never exceeded 3 %.

The corrected results are independent of the sampling length of the electron beam and of the initial gas density. The measurements of the normalized density are believed to be accurate to within ± 1 %. Owing to the uncertainty in the shock velocity and the pressure and temperature in front of the shock wave the length scale may be in error by ± 1·3%. The differentiated density profiles given in figures 1 and 9 and the reciprocal shock thickness may be wrong by approximately ± 4 %.

3. Argon shock waves

The measured density profiles in Ar shock waves for Mach numbers between 1·55 and 9·0 are shown in figure 1. The density is normalized in terms of the densities ρ_1 and ρ_2 in front of and behind the shock wave as indicated. The length scale is normalized by the mean free path λ_1 in front of the shock wave.† For low Mach numbers the shock is rather thick, the thickness reducing up to a Mach number of 3·4. For higher Mach numbers the thickness slightly increases again. For all Mach numbers the density profile is nearly symmetric. This can also be seen in the right-hand part of figure 1, where the normalized density gradient is plotted versus the reduced density. The maximum of these curves is identical with the reciprocal shock thickness.

† $\lambda_1 = \frac{16}{5}(\gamma/2\pi)^{\frac{1}{2}}\,\mu_1/\rho_1 a_1$, where γ = specific-heat ratio, μ = viscosity, ρ = density and a = speed of sound. Physical properties from NBS Circular 564 (1955) are $\lambda_1 = 1{\cdot}098$ mm for Ar at $T_1 = 300°$ K and $p_1 = 50$ mTorr.

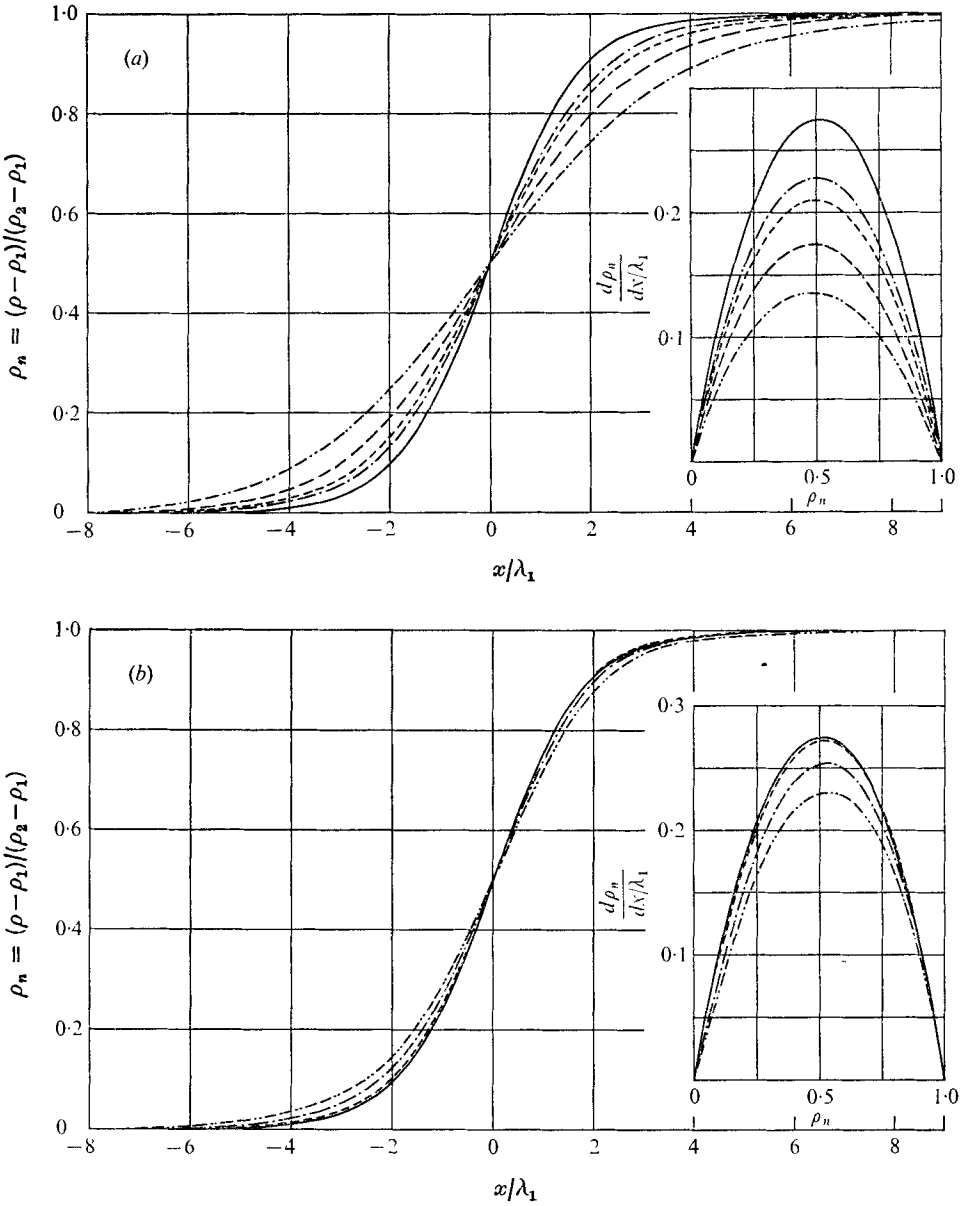

FIGURE 1. Measured density profiles in Ar shock waves. (*a*) - - — — - -, $M_S = 1{\cdot}55$; — — —, $M_S = 1{\cdot}76$; – – – –, $M_S = 2{\cdot}05$; - —— -, $M_S = 2{\cdot}31$; ——, $M_S = 3{\cdot}38$. (*b*) ——, $M_S = 3{\cdot}38$; – – – –, $M_S = 3{\cdot}8$; - —— -, $M_S = 6{\cdot}5$; - - — — - -, $M_S = 9{\cdot}0$.

The density profiles agree with those of Schmidt (1969) to within 1 % in the range $M_S = 2{\cdot}8$–$6{\cdot}5$, whereas for a Mach number of 8 the present results give a slightly lower density rise. These deviations are believed to be due to the improper absorption law used by Schmidt. The present profiles are within the experimental accuracy of the measurements of Schultz-Grunow & Frohn (1965) and Rieutord (1970).

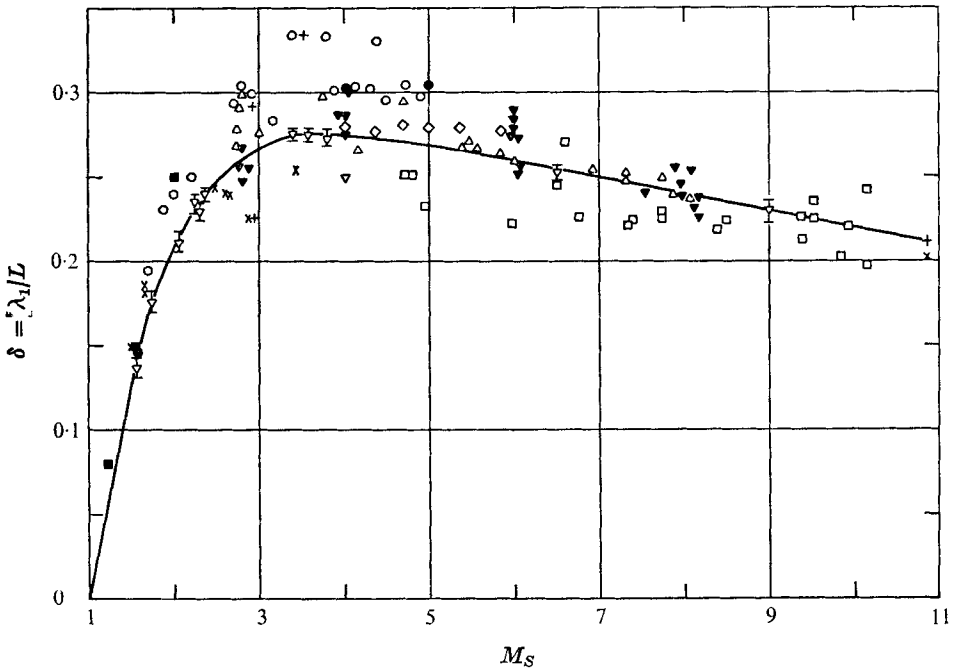

FIGURE 2. Reciprocal shock thickness in Ar, experimental results. □, Camac (1965); ■, Garen, Synofzik & Frohn (1974); ○, Linzer & Hornig (1963); ×, argon, Robben & Talbot (1966*a*); +, helium, Robben & Talbot (1966*a*); △, Russel (1965); ◇, Rieutord (1970); ▼, Schmidt (1969); ●, Schultz-Grunow & Frohn (1965); ▽, ——, present results.

In figure 2 the reciprocal shock thickness is plotted versus the Mach number. The error bars of the present results are given by the experimental scatter of at least three runs. Comparing the present results we find good agreement within the large scatter of other experiments.

For comparison with the predictions of various theories the full density profiles are used, as the shock thickness is characteristic of the central part of the shock wave only. The original computer program of Bird (1970) was used to compute the shock structure for all measured Mach numbers. This program simulates the flow by a set of several thousand particles and the intermolecular force law is assumed to be repulsive with $F \propto 1/r^{\nu}$. Excellent agreement is found for all Mach numbers if we set $\nu = 10$ (figure 3). Only for the lowest measured Mach number (1·55) do small deviations become visible. For the high energy intermolecular encounters taking place in the interior of a shock wave, the repulsive part of the intermolecular force law dominates the collision dynamics. Only for low Mach numbers may this situation change and the potential well and the attractive part of the potential become important for the collision processes within a shock wave. Probably, an attractive–repulsive force law in the Monte Carlo simulation would give better agreement with the experimental results for $M_S = 1{\cdot}55$ than a simple repulsive force law. Because of the very good agreement over the whole range of Mach numbers Bird's Monte Carlo simulation is believed to give an accurate description of the shock wave flow. The exponent $\nu = 10$ in the force law

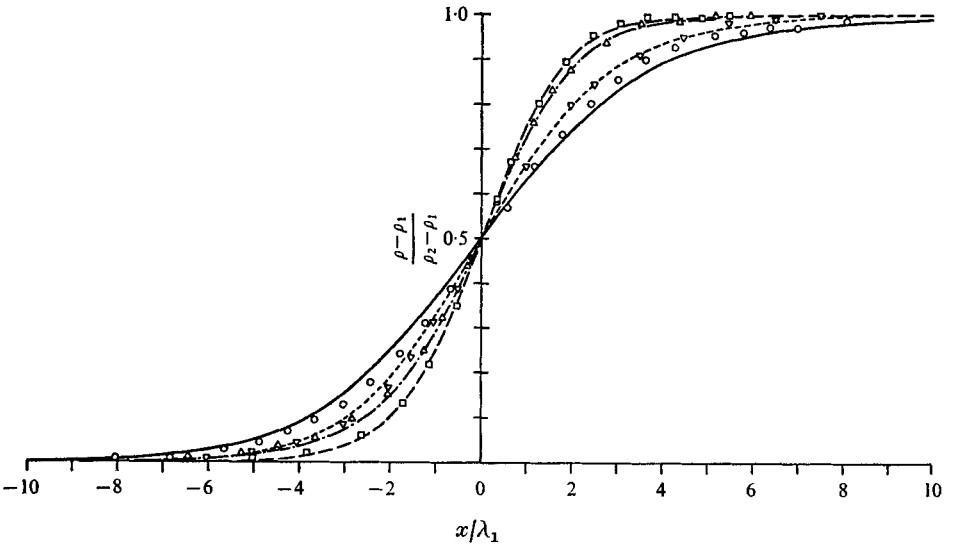

FIGURE 3. Comparison of measured and theoretical density profiles.

Shock Mach number	1·55	1·75	3·8	9·0
Monte Carlo (Bird 1970), $\nu = 10$	○	▽	□	△
Present experiments	——	- - - -	— — —	- —— -

corresponds to a viscosity–temperature relation $\mu \propto T^{\omega}$ with $\omega = 0{\cdot}72$. This relation reproduces the viscosity measurements of Guevara, McInteer & Wageman (1969) up to 2100 °K and viscosity calculations of Amdur & Mason (1958) based on molecular beam experiments. Schmidt found $\nu = 12$, but this result is based solely on his density profile for $M_S = 8{\cdot}0$. As mentioned above, this profile shows the largest deviations from the present results and seems to be slightly in error.

Calculations of shock structure for the Lennard–Jones, the exp-6 and simple repulsive intermolecular potentials, with Bird's Monte Carlo simulation, were carried out by Sturtevant & Steinhilper (1974) to determine the parameters in the potential models by adjusting the computed results to measured density profiles for $M_S = 8$. However the computed density profiles are very insentive to the different potentials at high Mach numbers. By using low Mach numbers, the shock profiles might give better information about the interaction law, especially about the potential well, as was discussed above.

The inverse-power interaction law with $\nu = 10$ is used to compare the present experiments with the Mott-Smith theory (Muckenfuss 1962) in figure 4. We find excellent agreement of the density profiles for Mach numbers up to $M_S = 6{\cdot}6$ (not presented here) and small deviations for $M_S = 9{\cdot}0$. Direct comparison of the Mott-Smith theory and Bird's Monte Carlo simulation for both density and temperature, as given in figure 5, again confirms that the Mott-Smith theory is better for lower than for higher Mach numbers. This result is contrary to the original assumptions of Mott-Smith (1951). The papers of Nathenson & Baganoff (1973) and Elliott & Baganoff (1974) also refer to the usefulness of the Mott-Smith solution for low Mach numbers. Furthermore it can be seen from figure 5 that the

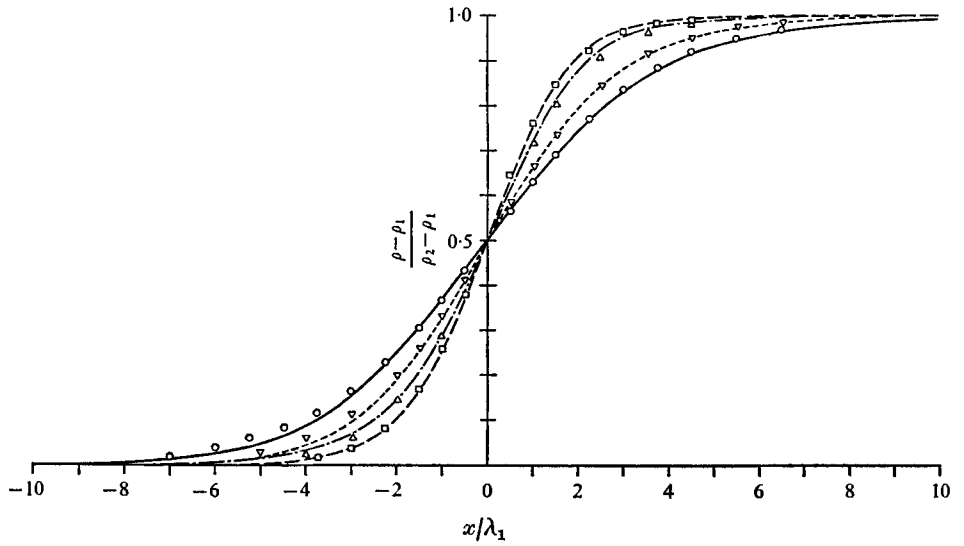

FIGURE 4. Comparison of measured and theoretical density profiles.

Shock Mach number	1·55	1·75	3·8	9·0
Mott-Smith (Muckenfuss 1962) $\nu = 10$	○	▽	□	△
Present experiments	——	– – – –	— — —	- —— -

temperature is a more sensitive quantity since it is a higher moment of the distribution function.

The Monte Carlo solution of the Boltzmann equation published by Hicks *et al.* (1972) for hard-sphere molecules is compared with the present results in figure 6. For low Mach numbers, this approach gives good agreement with experiment, but for higher Mach numbers the hard-sphere model gives too thin a shock wave. As shown by Yen & Ng (1974), the method yields thicker shock waves for softer molecules at high Mach numbers. Therefore better agreement may be expected for realistic molecules.

It is interesting to compare the measured low Mach number density profiles with the results of the Navier–Stokes theory, as this theory is generally supposed to be accurate for shock Mach numbers less than 2. But as can be seen in figure 7, significant deviations of the Navier–Stokes density profile are found even for $M_S = 1{\cdot}55$. The Navier–Stokes solution gives too thin a shock wave for all types of molecule (hard spheres, Maxwellian and realistic molecules, corresponding to $\omega = 0{\cdot}5$, 1 and 0·72 respectively). For higher Mach numbers increasing deviations are found. Also, the recent theories of Hicks *et al.* (1972) and Elliott & Baganoff (1974) predicted deviations of the Navier–Stokes shock profile from the real shock wave even for $M_S \leqslant 1{\cdot}2$.†

† In a paper by Garen & Frohn at the Thermodynamik Kolloquium, Karlsruhe, October 1975, measurements of Ar shock wave density profiles for $M_S = 1{\cdot}2$ with a laser differential interferometer were reported. These experiments again deviate from the Navier–Stokes density profile and are in agreement with the Mott-Smith profile. A summary of this colloquium will be published in *Brennstoff-Wärme-Kraft.*

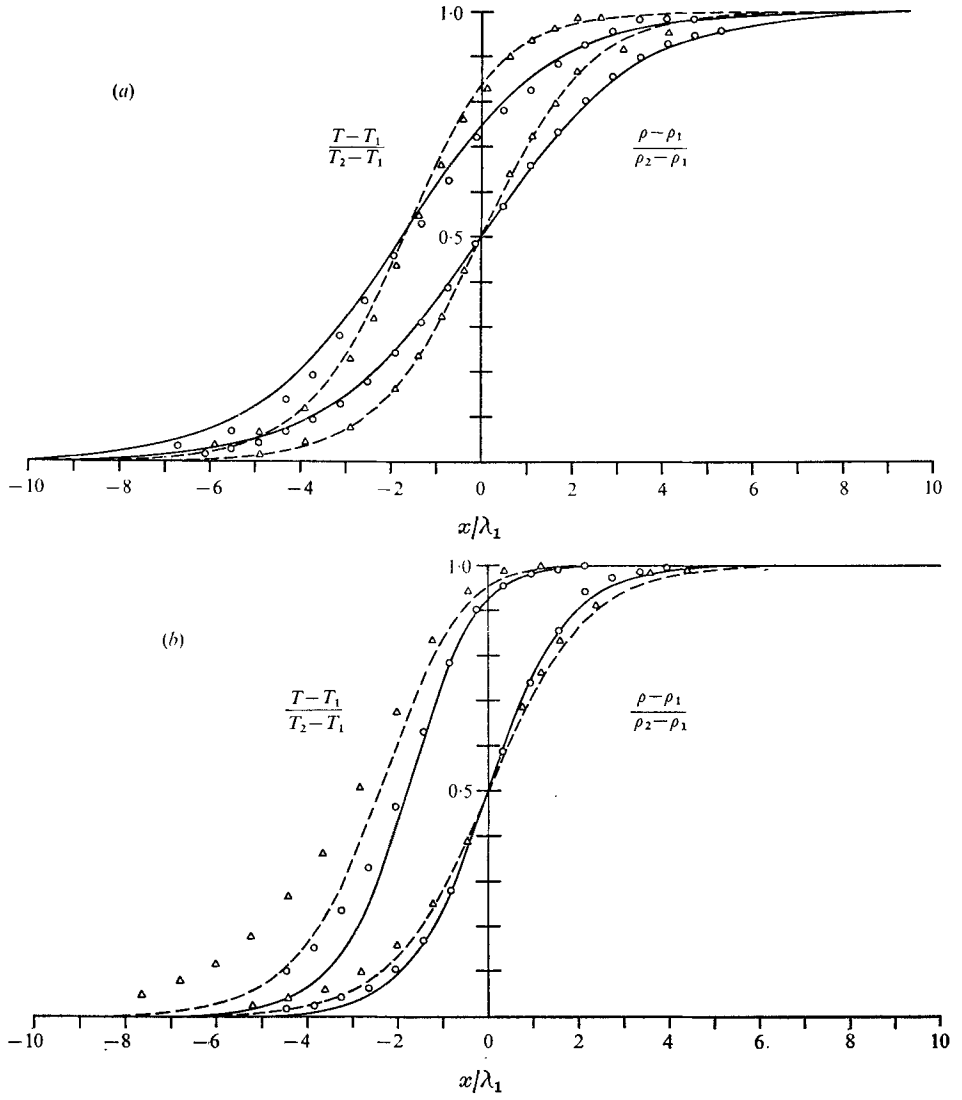

FIGURE 5. Comparison of theoretical temperature and density profiles.

	(a)		(b)	
Shock Mach number	1·55	2·05	3·8	9·0
Monte Carlo (Bird 1970), $\nu = 10$	○	△	○	△
Mott-Smith (Muckenfuss 1962), $\nu = 10$	——	— —	——	— —

For the Burnett equations, which are the second-order approximation of the Chapman–Enskog theory, numerical solutions are given by Foch (1973) for Mach numbers up to 1·9, using Maxwell molecules. For higher Mach numbers the Burnett equations fail to give any solution. The Burnett approximation for $M_S = 1{\cdot}55$ is in better agreement with the experimental results than the Navier–Stokes theory (figure 7) as it yields a lower density gradient. This is in accordance with the statement of Guiraud (1973) that the Burnett equations are able to give better

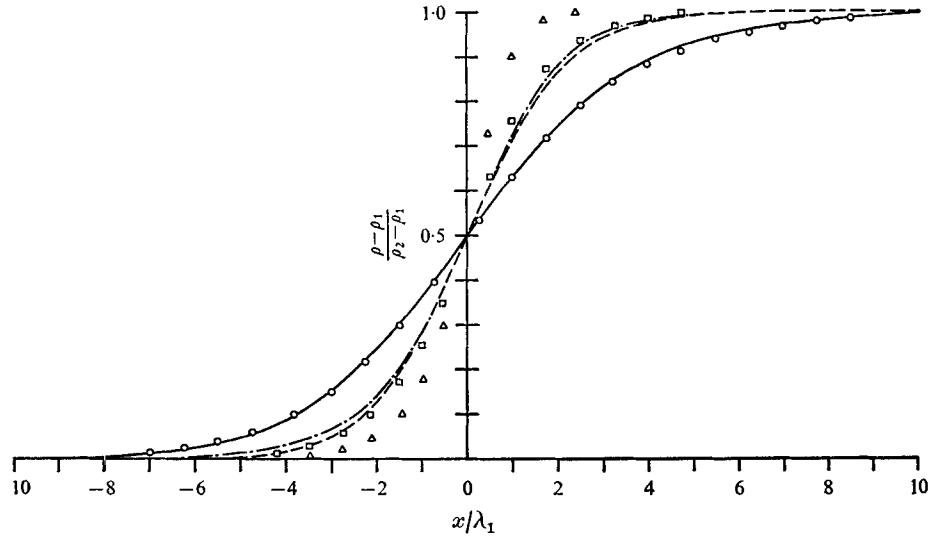

FIGURE 6. Comparison of measured and theoretical density profiles.

Shock Mach number	1·55	2·5	8·0
Hicks *et al.* (1972), $\nu = \infty$	○	□	△
Present experiments	——	— —	- ——-

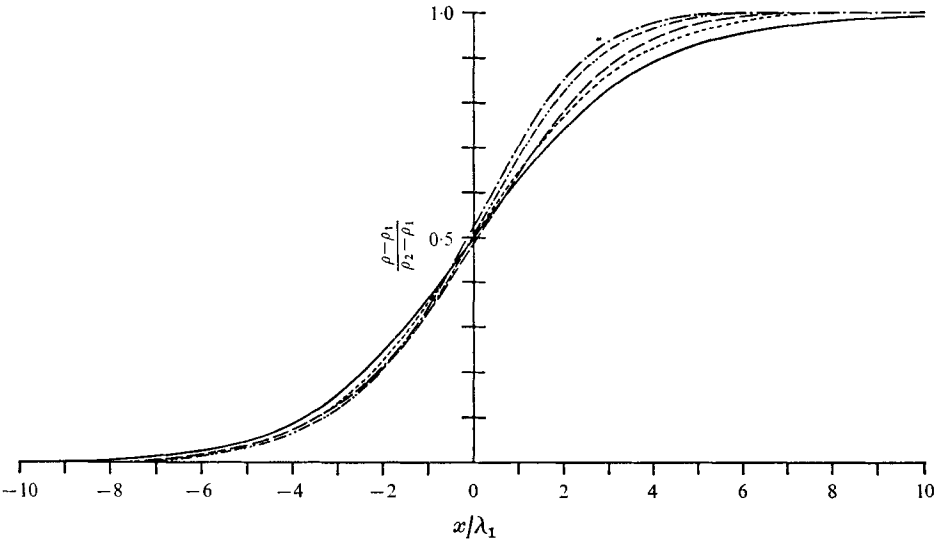

FIGURE 7. Comparison of the measured density profile with the Navier–Stokes and Burnett approximation for $M_S = 1{\cdot}55$. ——, experiment. Navier–Stokes: — —, $\omega = 1$ ($\nu = 5$); · · — — · ·, $\omega = 0{\cdot}72$ ($\nu = 10$); · ——— ·, $\omega = 0{\cdot}5$ ($\nu = \infty$). – – – –, Burnett (Foch 1973), $\omega = 1$ ($\nu = 5$).

accuracy when the Navier–Stokes solution is reasonably accurate but that they fail completely when the Navier–Stokes solution shows evident failure ($M_S > 1{\cdot}9$).

In figure 8 the asymmetry of the density profiles, defined as

$$Q = \int_{-\infty}^{0} \rho_n(x)\,dx \Big/ \int_{0}^{\infty} (1-\rho_n(x))\,dx,$$

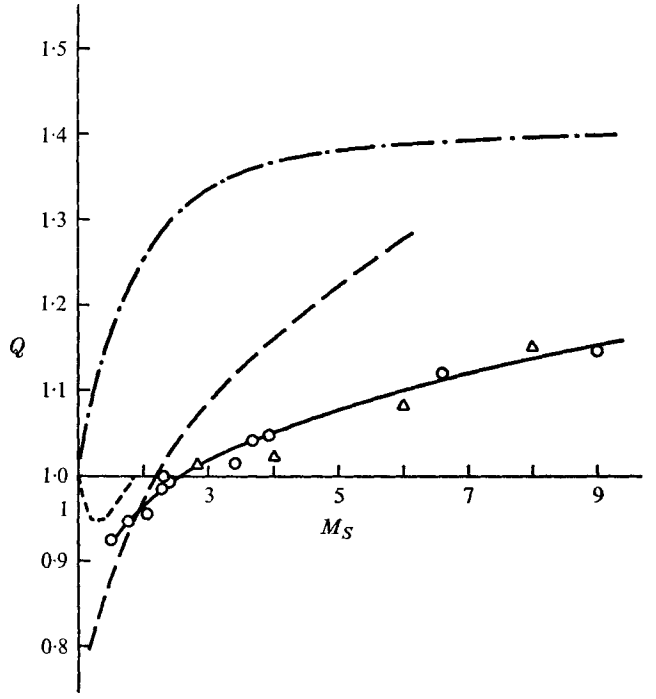

FIGURE 8. The asymmetry of the density profiles from experiments and theories. Theories: - —— -, Navier–Stokes, $\omega = 0{\cdot}72$ ($\nu = 10$); – – – –, Burnett (Foch 1973), $\omega = 1$ ($\nu = 5$); — —, Hicks *et al.* ($\nu = \infty$). Experiments: ——, △, Schmidt (1969); ○, present results.

as introduced by Schmidt (1969),† is plotted against the Mach number. The Navier–Stokes solution gives profiles which are too asymmetric, with $Q > 1$, whereas the Burnett approximation is in qualitative agreement with the experiments for low M_S, with $Q < 1$. The values of Q for the theory of Hicks *et al.* (1972) were recomputed from table 1 of that paper for hard-sphere molecules. The right qualitative behaviour is found, with $Q < 1$ for low M_S and $Q > 1$ for higher M_S. For more realistic molecules better quantitative agreement with the experimental results may be expected. The Mott-Smith solution is symmetric, with $Q = 1$ for all Mach numbers.

Some further theoretical models for the shock structure will be discussed briefly. The calculations of Baganoff & Nathenson (1970) are in satisfactory agreement with the measured density profiles for higher Mach numbers. But this theory gives too thin a shock wave for $M_S = 1{\cdot}5$, as it approaches the Navier–Stokes solution for $M_S \to 1$. The thirteen-moment solution of Grad (1952), which is restricted to $M_S < 1{\cdot}65$, and its modification by Butler & Anderson (1967) give too thick a shock wave. Furthermore the density profiles of Butler & Anderson are too asymmetric for high Mach numbers. The BGK model agrees with the Navier–Stokes solution for low Mach numbers and therefore disagrees with the experiment. For higher Mach numbers the BGK model yields too thin and too

† This equation differs from that used by Hicks *et al.* (1972) and Yen & Ng (1974) in the limits of the integrals.

asymmetric a profile, as has already been found by Schmidt (1969). The generalization of the BGK model proposed by Segal & Ferziger (1972) gives some improvement at high Mach numbers, but the agreement with experiment is not as good as for the Mott-Smith solution or the direct simulation method of Bird.

4. Nitrogen shock waves

Within N_2 shock waves additional relaxation of the rotational degrees of freedom takes place. The rotational relaxation here is strongly coupled to the translational relaxation. The measured density profiles for Mach numbers from 1·5 to 10 are given in figure 9. The normalization is the same as for the argon results. The N_2 density profiles are very similar to those in Ar: thick shock waves for low Mach numbers, decreasing shock thickness in the mean Mach number range up to $M_S = 6$ and for high Mach numbers a slightly increasing shock thickness. Here too the density profiles are nearly symmetric. This indicates the strong coupling of translational and rotational relaxation and suggests that the collision numbers for rotational and translational relaxation are of the same order of magnitude.

The present density profiles agree with the experimental results of Rieutord (1970) for $M_S = 6$. The experiments of Robben & Talbot (1966*b*), which were carried out in a hypersonic wind tunnel, are in good agreement with the present results for $M_S = 1{\cdot}7$, but give significantly thinner shock waves for high Mach numbers. Owing to the rapid expansion taking place in a low density hypersonic wind tunnel the population of the rotational energy levels ahead of the shock wave may deviate from the Boltzmann equilibrium distribution, as was found by Robben & Talbot. This may result in thinner shock waves in wind-tunnel experiments.

The reciprocal shock thicknesses from the present experiments are compared with the results of other measurements in figure 10. The error bars are given by the experimental scatter of at least three runs. Good agreement is found within the scatter of the other experimental results. A possible reason for the large deviations of the results of Robben & Talbot for high Mach numbers has been already mentioned above.

Several attempts have been made to describe the shock structure in a rotationally relaxing gas. When comparing the results of different theories with the present experiments some of the conclusions of the previous section on monatomic gases should be kept in mind.

The extended Navier–Stokes equation with additional bulk viscosity or a relaxation equation for the rotational energy transfer (Talbot & Scala 1961) gives too thin a shock profile. This even applies to the lowest measured Mach number, as has already been found for argon. There exist some kinetic model equations for diatomic gases which are based on the BGK model (Venkataraman & Morse 1969; Brau, Simons & Macomber 1969), but since the BGK model is found to be unsatisfactory for monatomic gases, agreement of the experimental results with these extended models is unlikely. The shock profiles of these model equations were obtained as approximate solutions, and by a suitable choice of the rotational

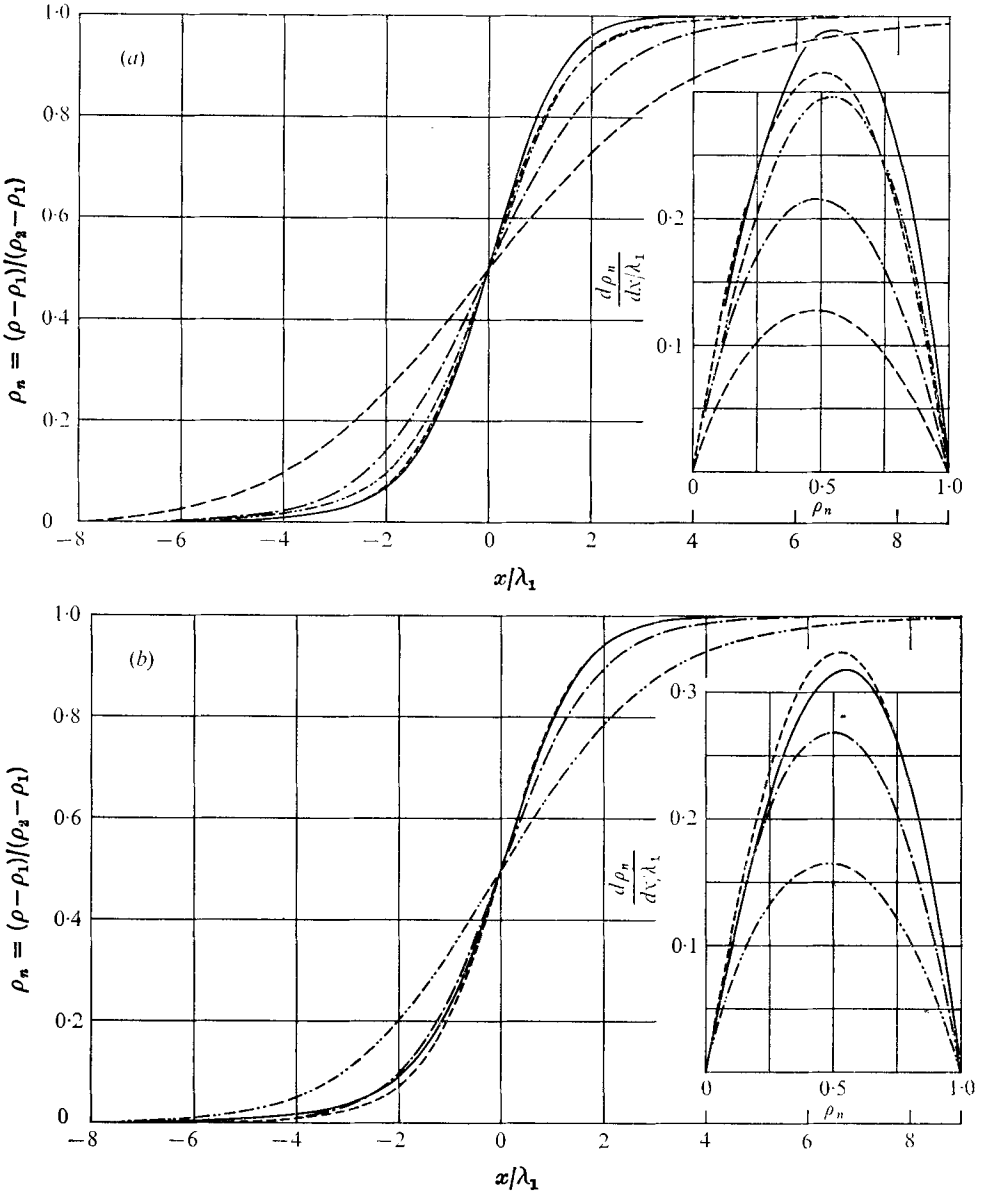

FIGURE 9. Measured density profiles in N_2 shock waves. (*a*) — —, $M_S = 1{\cdot}53$; - ——-, $M_S = 2{\cdot}0$; – – – –, $M_S = 3{\cdot}2$; ——, $M_S = 6{\cdot}1$; - - —— - -, $M_S = 10{\cdot}0$. (*b*) - - —— - -, $M_S = 1{\cdot}7$; - ——-, $M_S = 2{\cdot}4$; — —, $M_S = 3{\cdot}8$; ——, $M_S = 8.4$.

collision number agreement with experimental shock thicknesses can be obtained. However, the accurate numerical solutions of the same model equations by Giddens, Barbarika & Huang (1971) differ considerably from the approximate solutions of Venkataraman & Morse and give too thin a shock wave for all Mach numbers.

A modified Boltzmann equation with classical convex bodies of revolution as the colliding molecules was derived by Haight (1971). This model may describe

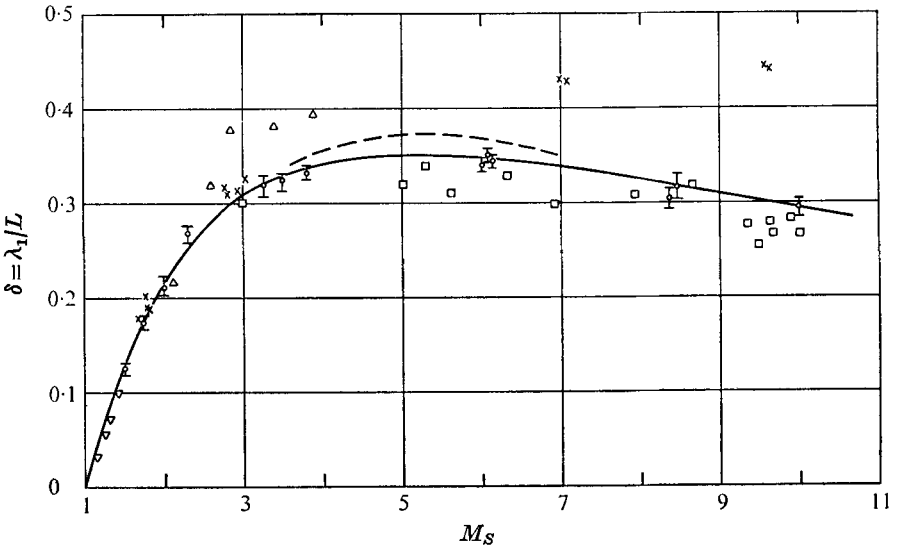

FIGURE 10. Reciprocal shock thickness in N_2, experimental results. □, Camac (1965); ▽, Greene & Hornig (1953); △, Linzer & Hornig (1963); — — —, Rieutord (1970); ×, Robben & Talbot (1966*a*); ——, ◇, present results.

well the shock structure of a rotationally relaxing gas. Calculations with this model equation should be carried out to compare with the present experimental results.

The Monte Carlo simulation of Bird (1970), which was found to be successful for monatomic gases, was extended by Bird (1971) to diatomic molecules. This 'energy sink model' takes into account the simultaneous energy transfer into translational and rotational degrees of freedom. The molecules are represented by point centres of repulsion ($F \propto 1/r^{\nu}$) and to each molecule an additional variable is allocated for the internal energy. The rotational energy transfer is described by a rotational collision number Z_R. The computer program of Bird was used to compute shock profiles for comparison with the present experimental density profiles. Very good agreement for all Mach numbers is found with $\nu = 9$ and $Z_R = 4$. But the temperature dependence of the shear viscosity from direct viscosity measurements in nitrogen yields a value of $\nu = 10$ for the large temperature range covered by the shock structure measurements. $\nu = 10$ corresponds to $\mu \propto T^{0.72}$.

The Monte Carlo simulation with $\nu = 10$ is in excellent agreement with the experimental density profiles (figure 11) if for high Mach numbers a slightly higher rotational collision number Z_R is used. Relating the mean temperature $\frac{1}{2}(T_1 + T_2)$ within the shock wave to the rotational collision number we find that $Z_R = 4$ corresponds to 300 °K and $Z_R = 5$ corresponds to 3200 °K. The strong temperature dependence of Z_R predicted by the theories of Parker (1959) and Lordi & Mates (1970) does not occur in our experiments, whereas $Z_R = 4$ for room temperature is confirmed. As was pointed out by Lordi & Mates (1970, p. 306), the disagreement may be due to the large differences in the rotational and translational temperatures within a strong shock wave.

The shock profiles calculated by the Monte Carlo simulation for density,

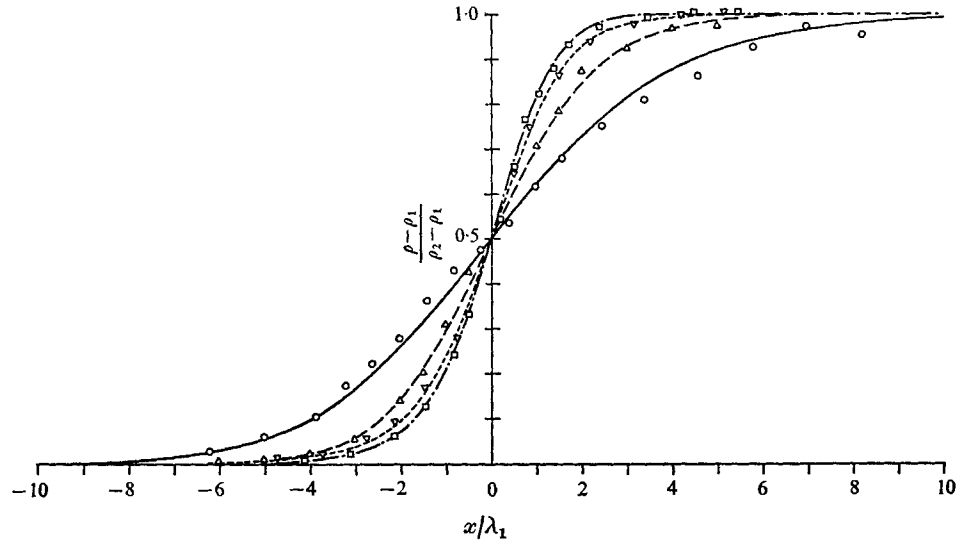

FIGURE 11. Comparison of measured and theoretical density profiles. Present experiment: ——, $M_S = 1{\cdot}53$; — —, $M_S = 2{\cdot}0$; - ——-, $M_S = 6.1$; – – – –, $M_S = 10{\cdot}0$. Energy sink model (Bird 1971), $\nu = 10$: ○, $M_S = 1{\cdot}53$, $Z_R = 4$; △, $M_S = 2{\cdot}0$, $Z_R = 4$; □, $M_S = 6{\cdot}1$, $Z_R = 4{\cdot}4$; ▽, $M_S = 10{\cdot}0$, $Z_R = 5$.

rotational temperature T_R and translational temperature T_T are presented in figure 12. The overshoot in T_T is clearly seen for high Mach numbers. For increasing M_S the rotational temperature profile moves further and further ahead of the density profile. This is in qualitative agreement with the measurements of Robben & Talbot (1966*b*).

5. Conclusion

Accurate density measurements have been carried out in argon and nitrogen shock waves for a large Mach number range. The argon measurements are in excellent agreement with the Monte Carlo simulation of Bird for a repulsive intermolecular force law. The Mott-Smith theory, employing the same force law, is in better agreement with the experiments for lower than for higher Mach numbers. This result is confirmed by direct comparison of the Monte Carlo and Mott-Smith results. Consequently, the Navier–Stokes approximation is expected to be less satisfactory even for low Mach numbers. This is indeed confirmed by the present experimental results for the lowest measured Mach number $M_S = 1{\cdot}55$. Thus the Navier–Stokes equations are violated even for very weak shock waves, as was pointed out by Elliott & Baganoff (1974) from analysis of the upstream and downstream singular points. The above may indicate that the distribution function within a shock wave is generally bimodal in character and that the distribution function of the first-order Chapman–Enskog theory does not apply to this type of non-equilibrium flow, even for low shock Mach numbers. However, the Burnett equation, the second-order Chapman–Enskog approximation, is in better agreement with the experiments, especially with respect to

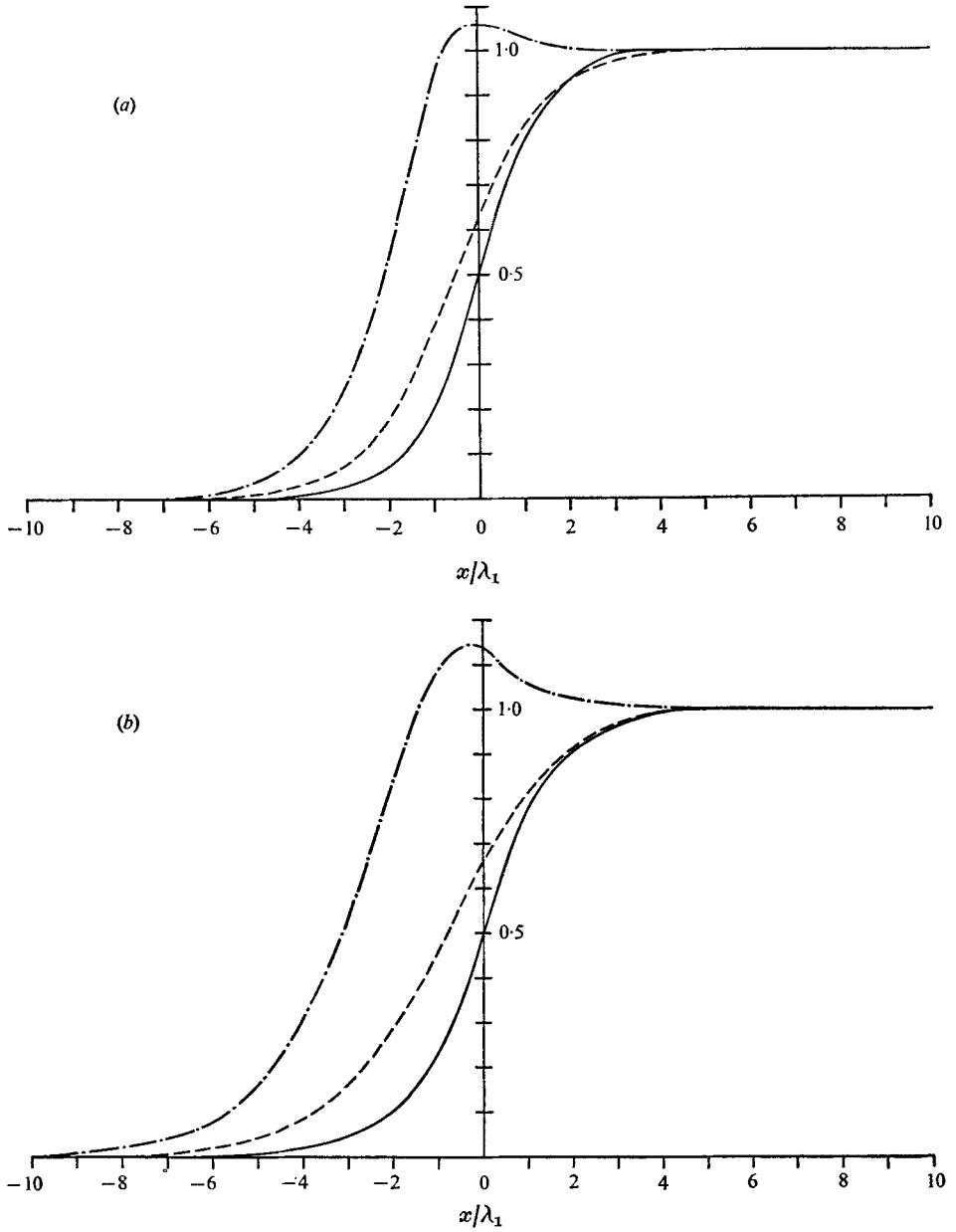

FIGURE 12. Temperature and density profiles in N_2 shock waves from the energy sink model (Bird 1971). ——, $(\rho-\rho_1)/(\rho_2-\rho_1)$; — —, $(T_R-T_1)/(T_2-T_1)$; - ——-, $(T_T-T_1)/(T_2-T_1)$. (*a*) $M_S = 2{\cdot}8$, $\nu = 10$, $Z_R = 4{\cdot}2$. (*b*) $M_S = 10.0$, $\nu = 10$, $Z_R = 5$.

the asymmetry of the density profiles. Some other models based on kinetic theory may be able to describe the shock structure in monatomic gases if a realistic intermolecular force law is used.

For molecular gases with rotational degrees of freedom, such as N_2, the theories suffer from the unknown rotational relaxation, which is strongly coupled to the

translational relaxation. Only the extended Monte Carlo simulation of Bird (1971), the 'energy sink model', was found to be in good agreement with the experimental density profiles for a realistic interaction law and a suitable rotational collision number. The rotational relaxation was found to be very fast even for strong shock waves with very high temperatures.

The author is greatly indebted to Professor B. Schmidt for providing the opportunity to conduct this research under his supervision, and for his encouragement and advice throughout the course of the work. The author is also grateful to Professor G. A. Bird for providing the computer programs for the Monte Carlo simulation. Special thanks are also due to Professor J. Zierep for his continued interest in the work and to Professor D. C. Pack for his helpful comments on the original manuscript. The calculations were carried out on the Univac 1108 computer of the Computing Centre of the University of Karlsruhe.

REFERENCES

ALSMEYER, H. 1974 Thesis, University of Karlsruhe, Germany.

AMDUR, I. & MASON, E. A. 1958 *Phys. Fluids*, **1**, 370.

BAGANOFF, D. & NATHENSON, M. 1970 *Phys. Fluids*, **13**, 596.

BIRD, G. A. 1970 *Phys. Fluids*, **13**, 1172.

BIRD, G. A. 1971 *Proc. 7th Int. Symp. on Rarefied Gas Dynamics*, vol. 2, p. 693.

BRAU, C. A., SIMONS, G. A. & MACOMBER, H. K. 1969 *Proc. 6th Int. Symp. on Rarefied Gas Dynamics*, vol. 1, p. 343.

BUTLER, D. S. & ANDERSON, W. M. 1967 *Proc. 5th Int. Symp. on Rarefied Gas Dynamics*, vol. 1, p. 731.

CAMAC, M. 1965 *Proc. 4th Int. Symp. on Rarefied Gas Dynamics*, vol. 1, p. 240.

ELLIOTT, J. P. & BAGANOFF, D. 1974 *J. Fluid Mech.* **65**, 603.

FOCH, J. D. 1973 *Acta Physica Austriaca*, suppl. 10, 123.

GAREN, W., SYNOFZIK, R. & FROHN, A. 1974 *A.I.A.A. J.* **12**, 1132.

GIDDENS, D. P., BARBARIKA, H. F. & HUANG, A. B. 1971 *Proc. 7th Int. Symp. on Rarefied Gas Dynamics*, vol. 2, p. 1051.

GRAD, H. 1952 *Comm. Pure Appl. Math.* **5**, 257.

GREENE, E. F. & HORNIG, D. F. 1953 *J. Chem. Phys.* **21**, 617.

GUEVARA, F. A., MCINTEER, B. B. & WAGEMAN, W. E. 1969 *Phys. Fluids*, **12**, 2493.

GUIRAUD, J.-P. 1973 *Proc. 13th Int. Congr. Theor. Appl. Mech.*, p. 104.

HAIGHT, C. H. 1971 *Proc. 7th Int. Symp. on Rarefied Gas Dynamics*, vol. 2, p. 1041.

HICKS, B. L., YEN, S. M. & REILLY, B. J. 1972 *J. Fluid Mech.* **53**, 85.

LINZER, M. & HORNIG, D. F. 1963 *Phys. Fluids*, **6**, 1661.

LORDI, J. A. & MATES, R. E. 1970 *Phys. Fluids*, **13**, 291.

MOTT-SMITH, H. M. 1951 *Phys. Rev.* **82**, 885.

MUCKENFUSS, C. 1962 *Phys. Fluids*, **5**, 1325.

NATHENSON, M. & BAGANOFF, D. 1973 *Phys. Fluids*, **16**, 2110.

PARKER, J. G. 1959 *Phys. Fluids*, **2**, 449.

RIEUTORD, E. 1970 Thèse, Lyon, France.

ROBBEN, F. & TALBOT, L. 1966*a* *Phys. Fluids*, **9**, 633.

ROBBEN, F. & TALBOT, L. 1966*b* *Phys. Fluids*, **9**, 653.

RUSSEL, D. 1965 *Proc. 4th Int. Symp. on Rarefied Gas Dynamics*, vol. 1, p. 265.

SCHMIDT, B. 1969 *J. Fluid Mech.* **39**, 361.

SCHULTZ-GRUNOW, F. & FROHN, A. 1965 *Proc. 4th. Int. Symp. on Rarefied Gas Dynamics*, vol. 1, p. 250.

SEGAL, B. M. & FERZIGER, J. H. 1972 *Phys. Fluids*, **15**, 1223.

STURTEVANT, B. & STEINHILPER, E. A. 1974 *Proc. 8th Int. Symp. on Rarefied Gas Dynamics*, p. 159.

TALBOT, L. & SCALA, S. M. 1961 *Proc. 2nd Int. Symp. on Rarefied Gas Dynamics*, vol. 1, p. 603.

VENKATARAMAN, R. & MORSE, T. F. 1969 *Proc. 6th Int. Symp. on Rarefied Gas Dynamics*, vol. 1, p. 353.

YEN, S. M. & NG, W. 1974 *J. Fluid Mech.* **65**, 127.